International Journal of Mass Spectrometry 305 (2011) 217–227

Contents lists available at ScienceDirect

International Journal of Mass Spectrometry

journal homepage: www.elsevier.com/locate/ijms

Degradation and oxidation postmortem of myofibrillar proteins in porcine skeleton muscle revealed by high resolution mass spectrometric proteome analysis

Bogdan Bernevic[a], Brîndușa Alina Petre[a], Dmitry Galetskiy[a], Carsten Werner[b], Michael Wicke[b], Karl Schellander[c], Michael Przybylski[a,*]

[a] Laboratory of Analytical Chemistry and Biopolymer Structure Analysis, Department of Chemistry, University of Konstanz, 78457 Konstanz, Germany
[b] Institute of Animal Breeding and Genetics, University of Göttingen, Germany
[c] Department of Veterinary Medicine, University of Bonn, Germany

ARTICLE INFO

Article history:
Received 16 August 2010
Received in revised form 2 November 2010
Accepted 8 November 2010
Available online 18 November 2010

Keywords:
High resolution proteomics
Myofibrillar muscle protein
FTICR mass spectrometry
Post-mortem degradation
Oxidative modification
2D-gel electrophoresis

ABSTRACT

Early postmortem changes of porcine muscle proteins including the rate and extent of pH decline, proteolysis and oxidation are key factors influencing the loss of water in meat, and proteolytic degradation may result in shrinking of muscle cells and drip loss. We report here the identification and structural characterisation of post-mortem degradation and oxidation of myofibrillar proteins using high resolution mass spectrometric proteomics. Soluble muscle proteins from *M. Longissimus dorsi* obtained 48 h postmortem at different drip loss were separated by two-dimensional gel electrophoresis (2D-PAGE), and degradation products were identified by Fourier-transform ion cyclotron resonance mass spectrometry. Oxidation products were detected by 2D-oxyblot analysis of 2,4-dinitrophenylhydrazine (DNPH)-treated proteins using an anti-DNP antibody, and selected spots were identified by liquid chromatography-tandem mass spectrometry (LC–MS/MS). Postmortem denaturation at low drip loss was found for four contractile proteins, myosin-light chain-1; myosin regulatory light chain; α-β-tropomyosin and α-actin. The combination of 2D-PAGE and FTICR-MS was found to be a powerful approach for identification of muscle protein degradation products, providing identification of several truncation forms of creatine kinase and troponin T. The comparison of 2D-oxyblot and silver-stained 2D-gels at low and high drip loss revealed approximately 70 oxidatively modified proteins from muscle cell lysate. Oxidative modifications, representing possible biomarker candidates, were identified at Lys-170 of creatine kinase (4-hydroxynonenal), Lys-326 of actin (amino-adipic semialdehyde), and at W-169 (kynurenine) of triosephosphate isomerase.

1. Introduction

Meat quality is a complex trait of processes that is influenced by genetic components, animal handling and environment, and slaughtering processes. Immediately after slaughter a shift in the biochemical processes occurs in muscle tissue as in all other organs, in response to the halt of the respiratory system and blood circulation. In muscle tissue, the morphological and ultrastructural changes as well as changes in energy metabolism have been well described and it is now known that the rate and extent of postmortem metabolic processes greatly influence important properties such as tenderness, water-holding and sensoric capacity of meat. Meat pH over a range of approximately 5–7.3 is significantly correlated to colour stability, water-holding capacity and microbiological stability [1]. It is generally accepted that degradation and denaturation of proteins during postmortem aging is responsible for the tenderization of meat [1]; e.g., activities of calpains and their inhibitors, calpastatins [2,3] have been associated with tenderization processes. Several structural proteins, such as actin, myosin, troponin T, and metabolic proteins such as glycogen phosphorylase, creatine kinase, and dihydrolipoamide succinyl transferase have been described to undergo *post-mortem* changes in *Longissimus dorsi* [4].

The rapid pH decline post-mortem causes denaturation (loss of functionality and water holding capacity) (WHC) of many proteins, and high rates of post mortem muscle glycolysis favor

* Corresponding author at: Laboratory of Analytical Chemistry, Department of Chemistry, University of Konstanz, Universitätstrasse 10, 78457 Konstanz, Germany. Tel.: +49 7531 882249; fax: +49 7531 883097.
E-mail address: Michael.Przybylski@uni-konstanz.de (M. Przybylski).

1387-3806/$ – see front matter © 2010 Published by Elsevier B.V.
doi:10.1016/j.ijms.2010.11.010

protein denaturation. Myofibrillar proteins are well suited for holding water because of its filament structure, and major changes in moisture retention originate in changes of the filament structure, resulting in denaturation of myofibrillar proteins [4,5]. Bendall et al. observed denaturation of sarcoplasmic proteins a low WHC, which was confirmed in subsequent studies [6,7]. From these data, a detailed proteomics study on denaturation and structural changes of myofibrillar and sarcoplasmic proteins at different pH and WHC appeared particularly interesting [8].

Metabolic processes in muscle tissue may lead to the formation of reactive oxygen species (ROS) and other oxidative products. Oxidative species including hydroxyl radicals, superoxide anion and nitric oxide can be detected by different methods. In *post-mortem* muscle tissue, when proteins are targeted by reactive oxygen species, this may result in carbonyl formation and decreased sulfhydryl levels; such modifications may alter the properties of meat proteins and quality of meat products [9]. Individual proteins and genes involved in protein carbonylation may be potentially useful biomarkers of protein oxidation caused either by the direct oxidation of amino acid side chains (e.g., proline and arginine to γ-glutamylsemialdehyde, lysine to aminoadipic semialdehyde, threonine to aminoketobutyrate), or via indirect reaction with oxidative by-products such as lipid peroxidation products (LPO) and advanced glycation end products (AGEs) [10,11]. Oxidative processes may also affect the water binding ability of membranes and contribute to drip loss [12]. A commonly used method of analyzing protein carbonyls is labeling with 2,4-dinitrophenyl hydrazine, thus forming a stable dinitrophenylhydrazone (DNP) product. DNP-labeled proteins can be analyzed by UV absorption or by using anti-DNP antibodies for ELISA or immunoblotting analysis [13,14]. A combination of methods of muscle protein fractionation, labeling of oxidation products, gel electrophoresis, and mass spectrometry has been employed in this study for the characterization of a structural modification and oxidation profile in porcine proteome.

A number of analytical methods have emerged in proteome analysis, including the development of rapid chromatography techniques [15], high resolution mass spectrometry [16,17], and fast search engines for sequence algorithm processing and data analysis. A frequently used method of protein identification from 2-DE is peptide mass fingerprinting by matrix-assisted laser desorption–ionization time-of-flight mass spectrometry (MALDI-TOF-MS). This technique allows identifications of femtomole quantities of peptides, but has shown limitations in applications to porcine proteins [18], most likely due to incomplete protein entries of the *Sus scrofa* genome database. Some difficulties in protein identification could be solved by combined liquid chromatography–electrospray ionization tandem mass spectrometry (LC–ESI-MS/MS), and by the use of additional taxonomies (human, bovine, sheep) [19]. The recent development of Fourier transform-ion cyclotron resonance mass spectrometry (FTICR-MS) has enabled a breakthrough for mass spectrometric biopolymer structure analysis and proteomics, using both ESI and MALDI ionization [20]. The high (low ppm) mass accuracy of FTICR-MS provides particular advantages for the identification of proteins with medium and low abundance, since only a small number of peptides is required for protein identification [21,22]. In combination with 2-DE, FTICR-MS peptide mixtures yield a series of masses with high accuracies suitable for protein identification from databases. In the present study a combination of methods of muscle protein separation, labeling of oxidation products, 2D gel electrophoresis, and mass spectrometry has been employed for the identification of postmortem protein degradation and oxidation products, and structure modifications in order to identify suitable biomarkers candidates.

2. Experimental procedures

2.1. Materials

IPG strips (3–10) were purchased from Bio-Rad (München, Germany). Carrier ampholytes (Servalyt 3–10) were from Serva (Heidelberg, Germany). Urea, thiourea, DTT, TEMED and Coomassie Brilliant Blue G were from Sigma (St. Louis, MO, USA). Solutions of 30% acrylamide/0.8% *N*,*N*′-methylenebisacrylamide, SDS, TCA, acetonitrile and ethanol were from Roth (Karlsruhe, Germany). Iodoacetamide, agarose and bromophenol blue were from Fluka (Buchs, Switzerland), CHAPS was obtained from Genaxxon Biosciences (Biberach, Germany); trypsin was purchased from Promega (Madison, WI, USA), OxyBlot™ Protein Oxidation Detection Kit from Chemicon (Temecula, CA, USA). All other chemicals were of analytical grade from Merck (Darmstadt, Germany).

2.2. Animals and tissue sample preparation

Samples were taken from *Longissimus dorsi* muscle between the 13th and 14th rib. Muscle pH, meat conductivity and meat colour groups were measured using Star-series equipment (Matthaeus, Köln, Germany). Muscle pH values determined 24 h post-mortem were 5.8 and 5.5, respectively. Drip loss was scored using a bag method by a size-standardised sample from *L. dorsi* collected 24 h post-mortem. The samples were weighted, suspended in a plastic bag, held at 4 °C for 48 h and weighted again at the end of holding time. Drip loss was determined as a percentage of weight loss based on the initial weight; drip loss values found were 0.7 and 5.1, respectively.

The snap-frozen pig muscle was weighted (average 150 mg) and kept at −80 °C until further work-up. Muscle sample were homogenized in two lysis buffers: (a) The strongly reducing lysis buffer 1 with the composition, 6 M urea; 2 M thiourea; 70 mM DTT; 4% CHAPS; 0.05% Servalyte (3–10); Complete Protease Inhibitor cocktail. (b) Lysis buffer 2 with the composition 50 mM Tris–HCl, pH 7.6; 150 mM NaCl, 1% (w/v) CHAPS, 1% (v/v) Triton X-100, 5 mM NaF, 2 mM activated Na_3VO_4 containing Complete Protease Inhibitor Cocktail. Weight-dependent (in mg) buffer volumes (in μL) were: lysis buffer: 9× sample weight; complete: 0.04× sample weight. After homogenization the samples were centrifuged at 4 °C for 20 min at 15,000 × *g* to remove unextracted cellular components and insoluble high-molecular weight proteins and protein complexes, and were then separated by 2-DE. The supernatant was removed and stored at −80 °C until use. Protein concentrations of muscle extracts were determined by both the Bradford method and the bicinchoninic acid (BCA) assay [23].

2.3. Two dimensional gel electrophoresis

IEF was carried out using a Multiphor horizontal electrophoresis system (Amersham Biosciences, Uppsala, Sweden) with 17 cm IPG strips (pH range 3–10) and sample being applied overnight using the in-gel rehydration method. The reswelling solution contained 7 Murea, 2 M thiourea, 4% CHAPS, 0.3% DTT, 2% Servalyt (3–10) and a trace of bromophenol blue. Rehydrated strips were run in the first dimension for about 30 kVh at 19 °C. After focusing, the IPG strips were equilibrated for 30 min in 6 M urea, 30% glycerol, 2% (w/v) SDS, 0.05 M Tris–HCl (pH 8.8), 1% (w/v) DTT and a trace of bromophenol blue, and were then run for further 30 min in the same solution except that DTT was replaced by 4.5% (w/v) iodoacetamide. The second dimensional separation was carried out with a Bio-Rad Protean II xi vertical electrophoresis system using 12% SDS-PAGE gels of 1.5 mm thickness. Strips placed on the vertical gels were overlaid with 1% (w/v) agarose in SDS running buffer (25 mM Tris–HCl, 192 mM glycine and 0.1% (w/v) SDS), and subjected to electrophore-

sis at 25 mA/gel for 30 min and 40 mA/gel until the tracking dye reached the anodic end of the gel. After separation in SDS-PAGE gels, the proteins were visualized by sensitive Colloidal Coomassie staining and scanned using a GS-710 calibrated imaging densitometer (Bio-Rad, München, Germany). Silver staining was performed as described [24] with a silver diamine staining solution (500 mM $AgNO_3$, 500 mM NH_4OH, 20 mM NaOH); a developer solution (citric acid (0.01%, w/v)/formaldehyde (0.1%, v/v)) was used to visualize the proteins, followed by stop solution (Tris base (5%, w/v)/acetic acid (2%, v/v)).

2.4. In-gel digestion and peptide extraction

Protein spots were excised, digested with trypsin and subjected to peptide extraction either manually according to Mortz et al. [25], or automatically using a DigestPro96 robot (Intavis Bioanalytical Instruments, Köln, Germany). For manual in-gel digestion and subsequent MALDI–MS analysis, the spots were excised and destained by addition of 60% acetonitrile in water for 20 min at 25 °C. After removal of supernatant and lyophilization of the gel spot, a solution of 50 mM NH_4HCO_3 was added for rehydration and incubated for 20 min at 25 °C. This procedure was repeated twice and the final rehydration was performed with the protease solution (12.5 ng/L trypsin in 50 mM NH_4HCO_3) at 4 °C for 45 min. The gel spots were then incubated for 12 h at 37 °C in 50 mM NH_4CO_3 and protein fragments were eluted for 3–4 h with 60% acetonitrile in water. The eluates were lyophilized to dryness and dissolved directly before MALDI–MS analysis in 5 μL acetonitrile:0.1% TFA in water (2:1).

2.5. MALDI–FTICR mass spectrometry

FTICR-mass spectrometric analysis was performed with a Bruker APEX II FTICR instrument equipped with an actively shielded 7 T superconducting magnet, a cylindrical infinity ICR analyzer cell, and an external Scout 100 fully-automated X–Y target stage MALDI source with pulsed collision gas (Bruker Daltonik, Bremen, Germany). The pulsed nitrogen laser is operated at 337 nm, and ions are directly desorbed into a hexapole ion guide situated one mm from the laser target. The device for pulsing collision gas in direct proximity to the laser target provides cooling of the ions, which have a kinetic energy spread of several electron volts when produced by the MALDI process. These ions are trapped in the hexapole where positive potentials at the laser target and at an extraction plate to help trap ions along the longitudinal axis. After a predefined trapping time the voltage of the extraction plate is reversed and the trapped ions are extracted for transmission to the ICR cell. Accumulation of ions from multiple laser shots in the hexapole before mass spectrometric analysis increases the sensitivity [26]. Ions generated by ten laser shots were accumulated in the hexapole for 0.5–1 s at 30 V and extracted at −15 V into the analyzer cell. A 100 mg/mL solution of 2,5-dihydroxybenzoic acid (DHB; Aldrich, Steinheim, Germany) in acetonitrile: 0.1% TFA in water (2:1) was used as the matrix. Aliquots of 0.5 μL of matrix solution and 0.5 μL of sample solution were mixed on the stainless-steel MALDI sample target and allowed to dry. Calibration was performed with a standard peptide mixture within an m/z range of approximately 5000.

2.6. LC–MSMS

LC–MS analysis was performed on a Esquire 3000+ mass spectrometer (Bruker Daltonik, Bremen, Germany) coupled to an Agilent 1100 binary pump system. LC separations were performed on a 1 mm × 10 cm Discovery Bio Wide Pore 3 μm C18 column (Sigma–Aldrich, Germany) using a flow rate of 50 μL/min. Peptides were eluted using a linear gradient from 98% solvent A (0.2% formic acid in water (v/v)) and 2% solvent B (0.2% formic acid in acetonitrile (v/v)) to 55% solvent B over 90 min. The electrospray source was operated in the positive ion mode with the following parameters: capillary voltage, 4.0 kV; capillary exit, 120 V. Nitrogen was used as both nebulizing (20 psi) and drying gas (9 L/min). The desolvation temperature was 300 °C. For MS/MS analysis, the instrument was operated in the data dependent mode such that a full scan spectrum was obtained followed by X MS/MS spectra obtained for the X largest ions observed in the proceeding full scan spectrum with an abundance above a specified threshold. Each MS was the sum of 6 microscans, and 20 microscans were collected for each MS/MS scan, for a maximal accumulation time of 200 ms. The intensity threshold triggering ion selection was 2×10^4. For MS/MS acquisition, the SmartFrag function of the ion trap was used, which ramps the fragmentation amplitude from 30% to 200% of the preset value (1.10 V). Eluting peptides were analyzed in the data dependent MS/MS mode over a 300–1200 m/z range. All peptides were selected for MS/MS analysis by collision-induced dissociation. Mass spectra were evaluated using the DataAnalysis 3.3 software package (Bruker Daltonics). MS/MS spectra were searched with SwissProt database using Mascot search algorithm allowing one missed cleavage site; carbamidomethyl was taken as fixed modification and oxidized methionine as variable modification.

High resolution LC–MSMS was performed with an LTQ-Orbitrap-MS (Thermo Scientific, Bremen, Germany equipped with a nanoelectrospray ion source (Proxeon Biosystems, Odense, Denmark). Peptides were separated with 100 min gradients from 5 to 40% acetonitrile in 0.5% formic acid. The data-dependent acquisition mode was employed. Survey MS scans were acquired in the orbitrap with the resolution set to a 60,000. Up to 5 most intense ions per scan were fragmented and analyzed in the linear trap.

2.7. Database search

Monoisotopic masses of all singly charged ions from the MALDI–FTICR mass spectra were directly used for database search procedures using BioTools software (Bruker Daltonik) in combination with MASCOT peptide mass fingerprinting search engine (http://www.matrixscience.com/cgi/nph-mascot.exe?1) or ProFound (http://129.85.19.192/profound_bin/WebProFound.exe). The database employed was NCBInr, a compilation of several databases including SWISS-PROT, PIR, PRF, PDB and GenBank CDS translations. Protein ID was assigned for the first candidate protein for each spot, using mammalian as taxonomy for protein identification. If the first candidate had the *Sus Scrofa* taxonomy, this protein was assigned. In the case the first candidate had a taxonomy similar to Sus Scrofa and the protein was not present in the Sus Scrofa database, the first candidate was selected. Due to the large number of sequences related to mammalian proteins, assignment of more than one protein in a single spot was not carried out.

2.8. Protein derivatisation with DNP and Western blot

To identify carbonyl groups introduced into amino acids side chains after oxidative modification of proteins, 2D-oxyblot analysis was performed as previously described [27]. Peptide derivatives produced by reaction with 2,4-dinitrophenylhydrazine (DNP) were immunodetected by an antibody specific to the DNP moiety attached to proteins using a commercial kit (Chemicon, Temecula, CA). Briefly, approximately 500 μg of muscle proteins solution was loaded on linear (3–10) IPG strips and isoelectrically focussed. The IPG strips were then placed in 15 mL test tubes and incubated for 20 min in 2 M HCl with 10 mM DNPH at 25 °C. After the reaction, the samples were washed for 15 min with 2 M Tris-base/30% glycerol. The IPG strips were then prepared for molecular weight separations as described above.

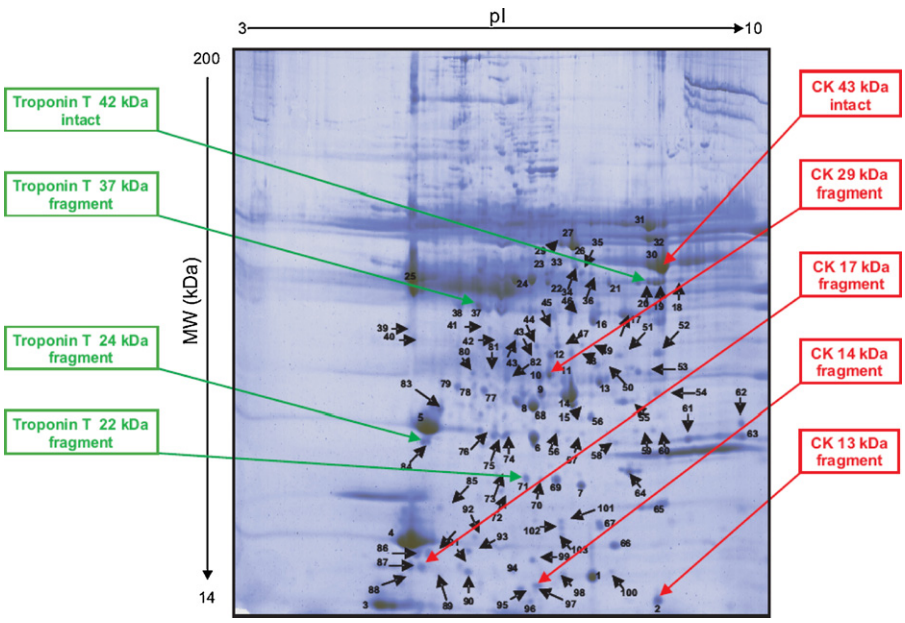

Fig. 1. Coomassie-stained 2D-gel electrophoresis of porcine *L. Dorsi* proteins taken 12 h postmortem, solubilized in denaturing lysis buffer. Arrows indicate the intact creatine kinase M and Troponin T, and their respective truncated forms.

The gels were transferred to a PVDF membrane using a wet transfer system (BioRad), and membranes were blocked for 1 h in a buffer containing 2.5% BSA in PBS and 0.5% Tween-20, pH 7.5, and then incubated for 1 h at 20 °C with a rabbit polyclonal anti-DNP antibody (1:300; Chemicon). The secondary antibody incubation was performed using horseradish peroxidase (HRP)-conjugated anti-rabbit IgG (1:600; Chemicon) for 1 h at room temperature. The immunoreactivity was visualized by enhanced chemiluminiscence using commercial reagents (Amersham Biosciences, Freiburg, Germany). The kit used for oxyblot analysis has a detection limit of approximately 10 fmol DNP residues. For estimation of specificity, the following oxidized proteins were included as positive controls: phosphorylase B, 97.4 kDa; bovine serum albumin, 68 kDa; ovalbumin, 43 kDa; carbonic anhydrase. 29.1 kDa; trypsin inhibitor, 21 kDa. For protein identification, spots were excised from the 2D-gels obtained with non-DNPH-treated samples and analyzed by mass spectrometry.

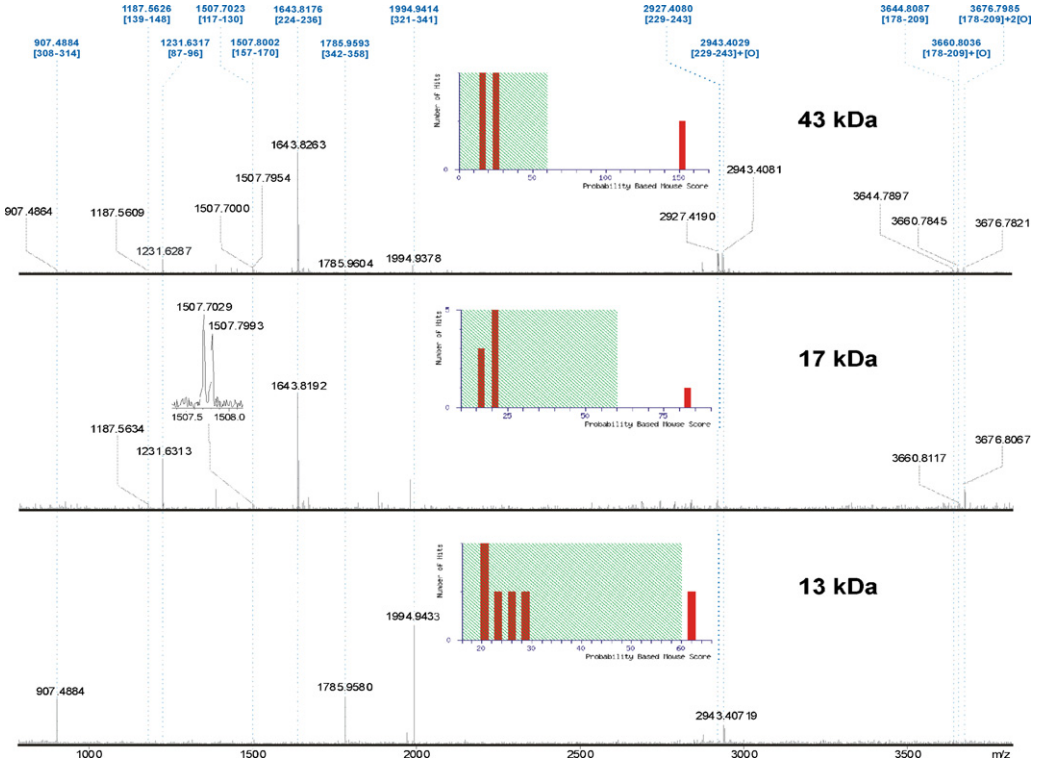

Fig. 2. Identification of intact creatine kinase M (43 kDa) and the CKM fragments at 17 and 13 kDa, respectively, by MALDI–FTICR MS peptide mass fingerprinting. The MASCOT database search results provided identification of the proteins with a probability based MOWSE score of >152.

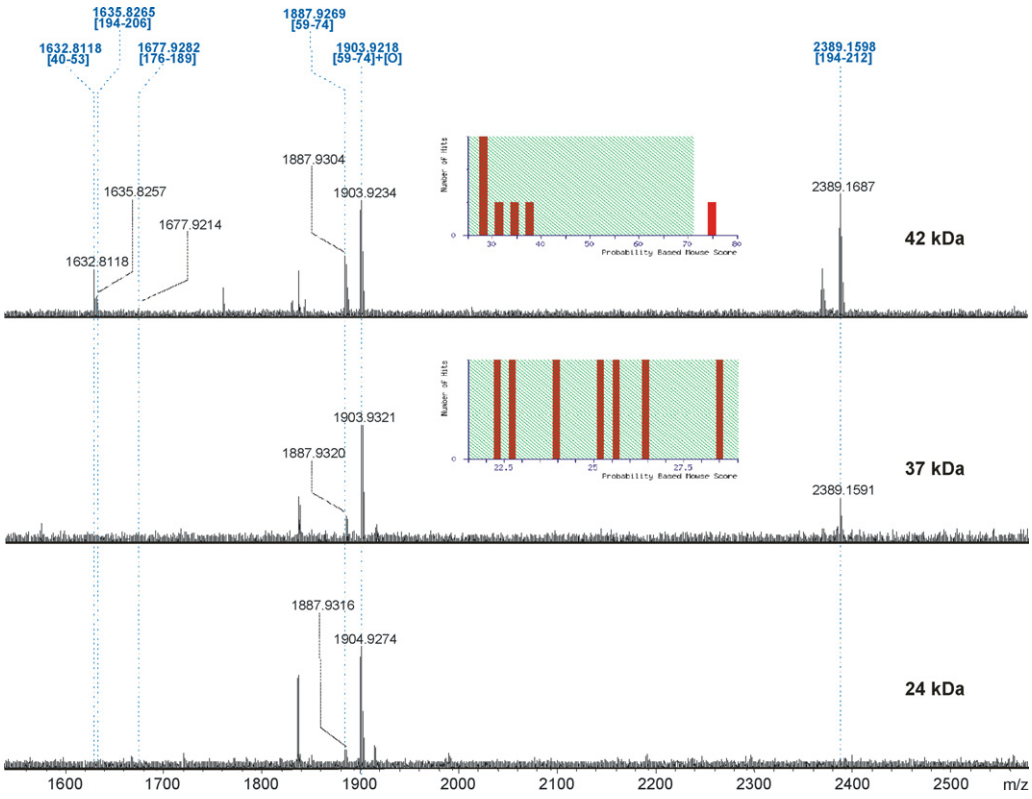

Fig. 3. Identification of intact Troponin T (42 kDa), and the troponin fragments at 37 and 24 kDa, respectively, by MALDI–FT-ICR MS peptide mass fingerprinting. The MASCOT database search results provided identification of the proteins with a probability based MOWSE score of >85.

3. Results and discussion

3.1. Separation and identification of porcine muscle proteins

Two different lysis buffers for muscle tissue were initially tested in order to evaluate the efficiency of solubilization and reproducibility of gels. Approximately 400 μg of muscle proteins obtained 12 h postmortem were reduced, alkylated and separated by 2D gel electrophoresis using a pH gradient of 3–10 (Fig. 1). The use of strongly reducing-denaturing buffer (see Section 2) provided good solubilization of structural proteins and contractile proteins, including constituents of the actomyosin complex (α- and β-tropomyosin, actin, troponin, myosin heavy and light chains); two isoforms of myosin light chains 1 and 2 were identified (Fig. S1 and Supplementary Table S1). A further abundant protein in muscle was identified as creatine kinase which is bound to myosin and localized at the M band of the sarcomere [28] It has been demonstrated to be functionally coupled to myosin ATPase and serves as an important myofibrillar ATP-regenerating system [29]; hence, changes in myofibrillar creatine kinase activity may disturb energy utilization and result in contractile dysfunction.

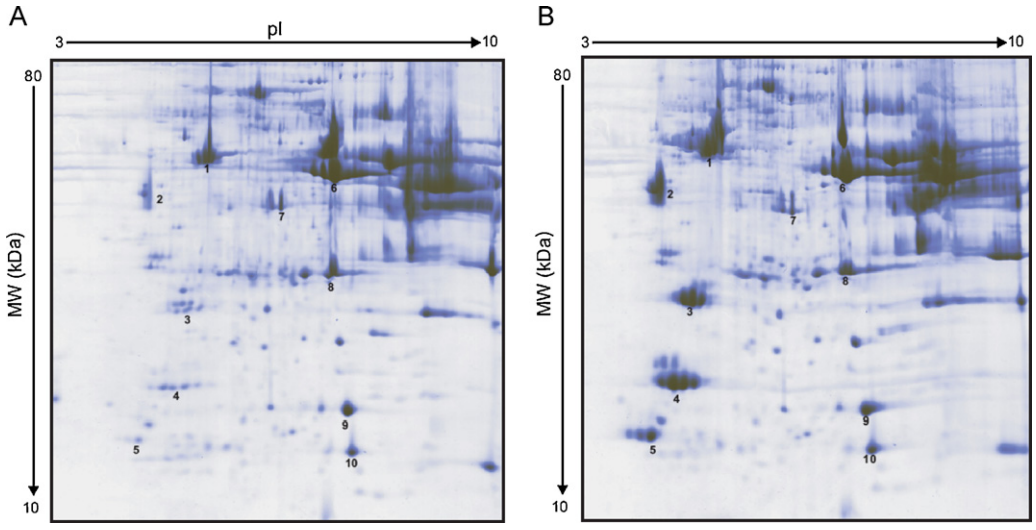

Fig. 4. Coomassie stained high resolution 2D-gel electrophoresis of porcine *L. Dorsi* proteins taken 48 h postmortem, showing the comparison of contractile proteins of (A) low pH (high drip loss) and (B) high pH (low drip loss).

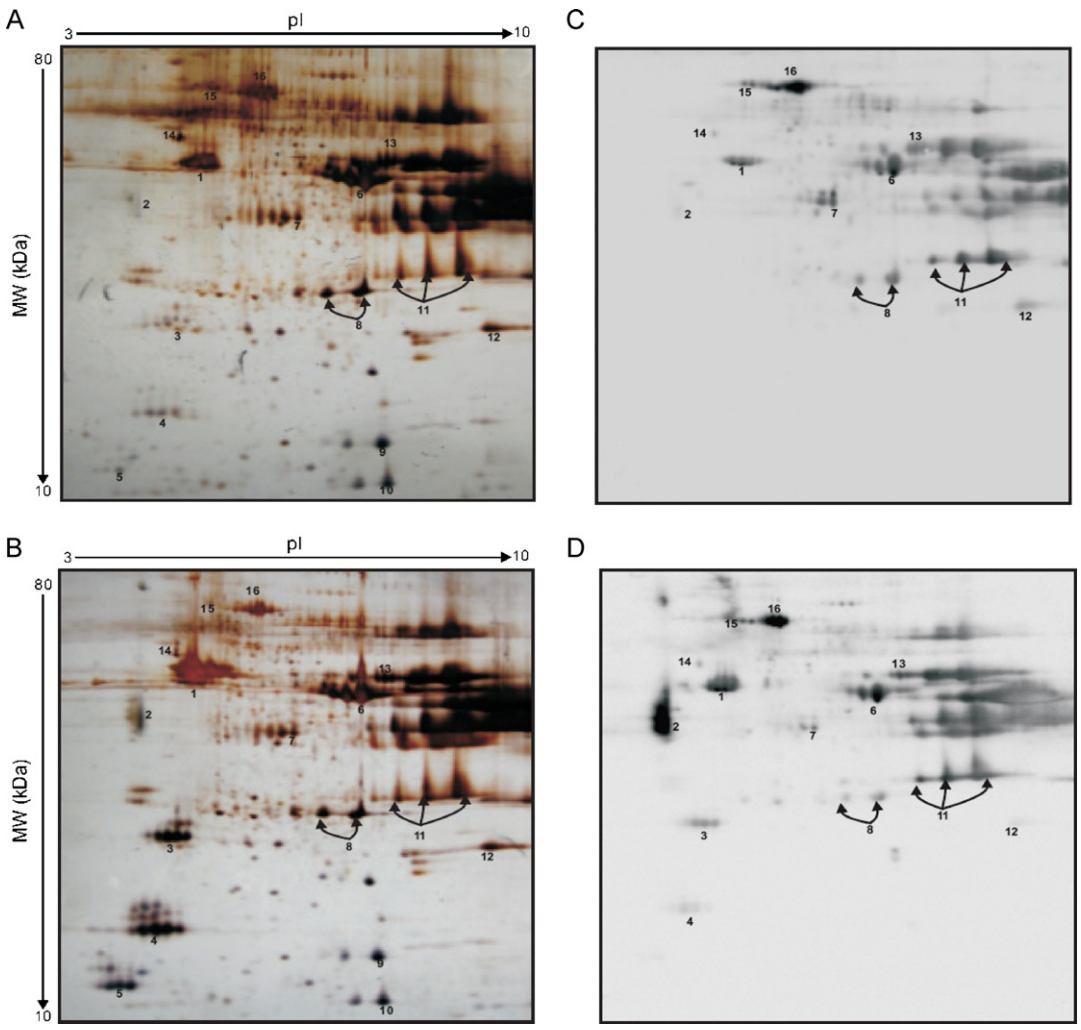

Fig. 5. Silver-stained 2D gel electrophoresis of muscle proteins 48 hrs postmortem at high drip loss (A) and low drip loss (B), and corresponding immunoblots (C and D) of DNP-labeled carbonylated muscle proteins. The proteins were separated by use of linear (3–10) IPG strips, followed by size separation on 12.5% SDS-PAGE, and subsequently blotted to a PVDF membrane as described in Section 2.

In contrast, the use of a non-denaturing lysis buffer provided better solubilization of cytoplasmic and soluble proteins involved in different metabolic pathways of skeletal muscle, and a better reproducibility of the gels. The majority of these proteins were also separated by 1D gel electrophoresis in biopsy samples, and 12 and 24 h postmortem (data not shown). Soluble proteins have been previously studied in diseased muscle, particularly creatine kinase; other soluble proteins were previously found in pathophysiological states including carbonic anhydrase III, enolase, phosphoglycerate mutase, pyruvate kinase and mitochondrial ATP synthase [30,31].

For identification of proteins separated by 2D-electrophoresis (see Fig. 1), gel spots were excised, destained, digested with trypsin, and proteolytic peptides extracted and analyzed by high resolution MALDI–FTICR-MS. Intact and/or truncated proteins identified by FTICR-MS are summarized in Supplementary Table S1 (see Supplementary Material). The high resolution FTICR-MS analyses generally provided identifications of proteins with mass determination accuracies <approx. 8 ppm (typically 4–6 ppm) by peptide mass fingerprinting, using mammalian as taxonomy due to the incomplete genomic data for porcine proteins, and ID assignment was made for the first candidate protein of each spot as described in Section 2. At these conditions, the high resolution mass spectrometric analysis provided the identification of approximately 70 proteins with one or several truncation forms (Fig. 1 and Supplementary Table S1). The large number of sequences related to mammalian proteins by using the NCBInr database increased the number of peptides required for identification. In contrast, using the SwissProt database containing sequences of intact proteins and precursors, the minimum number of peptides required for protein identification was found to be strongly dependent on the molecular weight of the protein. In both cases, the high mass accuracy of FTICR-MS provided an efficient tool for identification of truncated protein forms.

3.2. *Identification of post mortem truncation forms of muscle proteins*

A number of truncation forms in addition to the intact proteins and isoforms was identified by MALDI–FTICR-MS peptide mass fingerprinting (see Supplementary Table S1). Proteolytic truncation may result from the action of calpain proteinases which, however, were not directly observed in 2D-gels, due to their very low abundance. The identification of creatine kinase M (CKM) and two CKM truncation products using the MASCOT search engine and SwissProt database is illustrated in Fig. 2. Truncation products of CLM may result from cleavage by calpains [2,3]; however no structural details have been reported, and calpains were not observed in 2D-gels due to their low abundances. An intact isoform of CKM (mol. weight, 43 kDa) was identified with a MOWSE score of 152 in gel spot 30, pI 8.7 (Fig. 1) by 13 tryptic peptides covering approximately

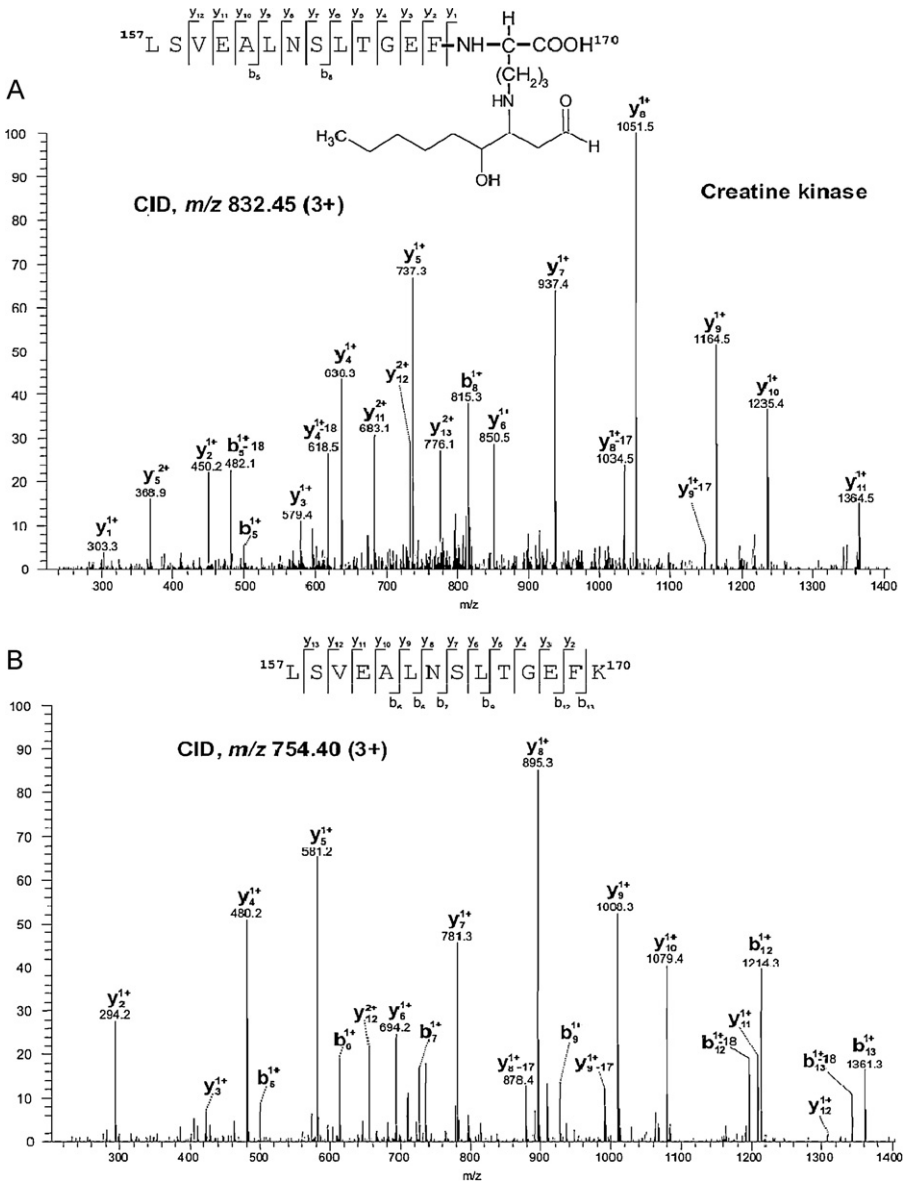

Fig. 6. Positive ion nano-HPLC-ESI/MS of N-hydroxynonenal-modified and non-modified creatine kinase tryptic peptides LSVEALNSLTGEFK from high pH muscle sample. MS spectra averaged over the chromatographic window where peptides were eluted (51.87 min and 54.80 respectively). (A) CID spectrum of precursor ion *m*/*z* 832.45 (3+), showing modified peptide (157–170) of full length creatine kinase, containing the Lys-HNE modification site at K-170 with a mass shift of 156. (B) CID spectrum of precursor ion *m*/*z* 754.40 (3+), showing non-modified peptide 157–170 of full length creatine kinase.

40% of the protein sequence (Fig. 2A). In Fig. 2B and C the identification of two truncation products with molecular weights of 17 and 13 kDa is shown, with sequences corresponding to residues (87–236) and (267–358), respectively, which represent proteolytic cleavage of CKM between residues 237 and 266. The identification of a 17 kDa C-terminal truncation product (gel spot 87; pI 5.4) was obtained by 7 tryptic peptides. At the mass resolution used (approximately 100,000), two adjacent peptides with the mass difference <0.1 Da could be separated, one of which (*m*/*z* 1507.7029) was identified as the partial sequence, ^{117}GGDDLDPNYVLSSR^{130}, while the second peptide (*m*/*z* 1507.7993) had the sequence, ^{136}SIKGYTLPPHCSR^{148}. An N-terminal truncation product of CKM (mol. weight 13 kDa) was identified in gel spot 97 at a pI of 8.6 (Fig. 2C). The identified peptides of the truncation products covered 20% of the intact protein sequence with mass accuracies <3 ppm.

Several truncation products of contractive proteins were also identified. However, contractive proteins were generally characterized by a larger number of protein isoforms found by 2-DE, and a smaller number of tryptic peptides due to the higher proteolytic stabilities of structured sequence domains. Fig. 3 shows the identification of Troponin T and two of its truncation products. Intact Troponin T fast skeletal muscle isoforms (mol. Weight 42 kDa) was identified in gel spots 20 and 21 (pI 8.3) (Fig. 3A) with a MOWSE score of 85. The presence of these isoforms with different pI values may be due to post-translational modifications such as phosphorylations which, however, were not identified in the present study. An N-terminal truncation product of Troponin T was identified in gel spot 37 (pI 6.3) with a molecular weight of 37 kDa. A further truncation form at pI 5.6 with a molecular mass of 24 kDa could not be directly assigned using the MASCOT search engine. However, the high resolution mass spectrometric determination of the peptides *m*/*z* 1887.9316 (^{59}DLMELQALIDSHFEAR^{74}; mass accuracy, 2.5 ppm), and the same fragment at *m*/*z* 1903.9274 (modified by oxidation at Met-61; mass accuracy 0.8 ppm) provided evidence for the identification of this protein fragment as an N- and C-terminal truncation product of Troponin T. The exact N-terminal sequences of both the creatine kinase and Troponin T truncation products are

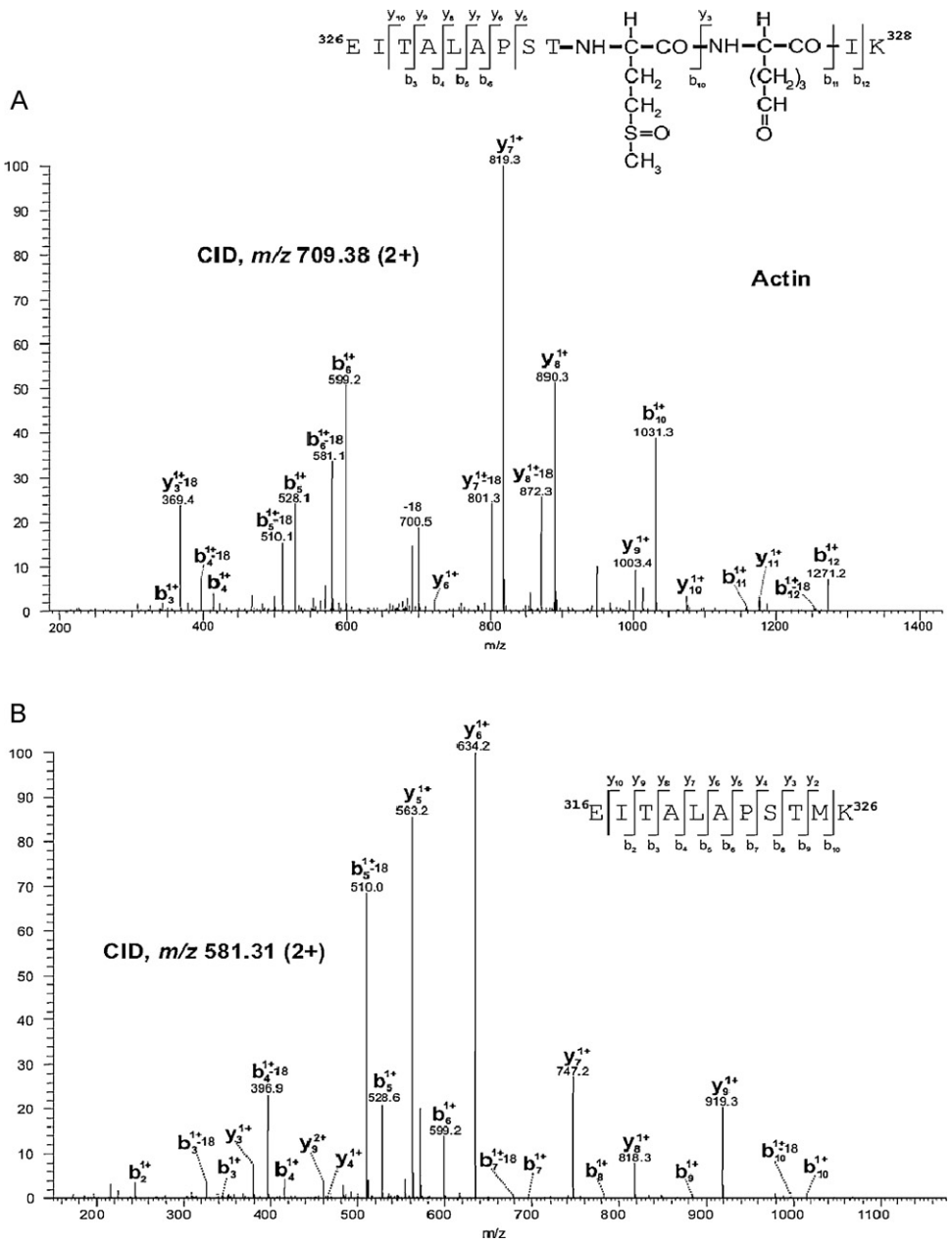

Fig. 7. Positive ion nano-HPLC-ESI/MS of Lys-326 oxidized actin tryptic peptide (EITALAPSTMKIK) (316–328) from the muscle sample isolated at high pH. Mass spectra were averaged over the chromatographic window where the peptide was eluted (30.92 min). (A) CID spectrum of precursor ion *m*/*z* 709.38 (2+), showing modified peptide (316–328) of full length α-actin, containing oxidation site at K-326 with a mass shift of 15 amu corresponding to the aminoadipic formation. (B) Spectrum of unmodified peptide (316–326).

currently determined by Edman sequencing of the proteins isolated from the gels.

Some limitations of protein identifications were noted in using SwissProt/NCBInr databases, containing large amounts of mammalian proteins without taxonomy specification. These limitations in isoform assignment may be overcome by creating a subject-specified database using high-accuracy peptide masses determined by high resolution FTICR-MS, and matching by database search in intact protein isoforms. Such databases may also facilitate the identification of degradation products 2D-gel spots.

3.3. Identification of denatured muscle proteins at different post-mortem pH

In order to characterize possible differences in solubilities of muscle proteins, proteins were extracted from *L. dorsi* from samples at high and low drip loss, using the same lysis buffer (see Section 2). After homogenization of muscle samples and centrifugation, protein concentrations were determined. Although in both cases identical ratios of lysis buffer to muscle protein were used, the protein concentration at low drip loss was significantly higher, which may be explained by increased denaturation at high drip loss due to the lower pH. A combination of 2D gel electrophoresis and 2D Western blot was used to characterize a possible correlation of denaturation of proteins with the extent of oxidation. Soluble protein extract was separated by 2-DE at pH 3–10 IPG strips on a 12% gel, and gels stained with Coomassie Brilliant Blue. The comparison of the 2 D-gels showed a significant increase of denatured proteins at low pH (high drip loss) in comparison to the protein sample at low drip loss (high pH) (Fig. 4A and B).

For protein identification the corresponding spots were excised, digested with trypsin and subjected to LC–MS/MS analysis. The

Table 1
Muscle proteins with significant changes at low and high drip loss (high/low pH) identified by LC–MSMS.

Spot	Protein	pI	Mw (KDa) gel	Peptides identified	Sequence coverage %	Protein accession no.
1[a]	Alpha-actin	5.3	42	47	77	P68137
2[a]	Tropomyosin	4.6	32	10	27	P07951
3[a]	Myosin light chain 1	4.9	21	18	29	P02602
4[a]	Myosin regulatory light chain 2	4.8	19	22	84	P97457
5[a]	Myosin light chain 3	4.6	16	18	38	P02602
6[b]	Creatine kinase M chain	6.6	43	64	60	Q5XLD3
7[b]	GAPDH	5.8	38	23	41	P00355
8[b]	Triosephosphate isomerase	6.4	26	54	69	Q29371
9[b]	Myoglobin	6.7	17	70	74	P02189
10[b]	Hemoglobin beta chain	7.1	16	83	87	P02067

[a] Myofibrillar proteins.
[b] Sarcoplasmic proteins.

results showed predominant denaturation of myofibrillar proteins at low pH (high drip loss), while sarcoplasmic proteins were essentially unchanged (Table 1). From approximately 250 protein spots, only 5 contractile proteins (actin, actinin, myosin regulatory light chain and light chain 1, tropomyosin) were found to be denatured.

3.4. Relationship of carbonylation and drip loss of muscle proteins

Postmortem changes in muscle proteins are accompanied by a pronounced increase in oxidation, particularly increased oxidation of myofibrillar proteins [32]. Proteins were separated both by SDS-PAGE and 2-DE with the aim to compare the extent of oxidized (carbonylated) proteins in muscle at high and low drip loss. Oxidized SDS-PAGE and 2-DE gel profiles were obtained by derivatization of protein carbonyl groups with DNPH reagent and immunostaining with anti-DNP antibody. Immunolabeling of muscle proteins 48 h postmortem separated on SDS-PAGE established the presence of carbonylated proteins in porcine muscle; the specificity of immunoblots was confirmed by staining with DNP-antibody in the absence of DNPH-derivatisation reagent (data not shown).

A detailed pattern of protein composition and carbonylation products was obtained by 2-DE and 2D-immunoblotting of muscle proteins (Fig. 5). The level of protein carbonylation was investigated in proteins at 48 h postmortem at low and high drip loss by identifying oxidized proteins through 2D-oxyblot analysis. In contrast to SDS-PAGE the DNPH reagents contain salts and detergents that must be removed prior to IEF. Thus, the addition of SDS to the derivatization reaction with DNPH is essential, but SDS is detrimental to IEF due to its protein binding and charge modification. In the present study, a modified approach was applied with the DNPH-derivatization performed subsequent to IEF, by derivatization directly in the IPG strips immediately followed by IEF. By comparison of 2D-oxyblots and silver-stained 2D gels, approximately 70 protein spots (of ca. 250) were found to be oxidatively modified (Fig. 5). Significant differences were observed in the extent of protein carbonylation in samples at low and high drip loss (Fig. 5C and D), showing higher abundances of carbonylation for contractile proteins at low drip loss (actin, myosin, tropomyosin). By contrast, no difference at low and high drip loss was observed for proteins with strong oxyblot response (e.g., serum albumin, creatine kinase M, triosephosphate isomerase).

3.5. Identification of oxidative modifications in muscle proteins

Because the derivatisation with DNPH is expected to affect the background and sensitivity of the mass spectrometric analysis of isolated proteins, proteins spots to be analyzed by mass spectrometry were excised from parallel 2D-gels obtained from non-DNPH-treated protein samples, separated in identical manner. Protein spots were excised from the gels, destained and digested with trypsin as described in Section 2. Approximately 30 oxidized proteins were identified by LC–MS/MS from 2D-gels; characteristic full length proteins are summarized in Table 2. Identifications of modification sites by MS/MS analysis of tryptic peptide fragments are illustrated in Figs. 6 and 7 for creatine kinase and actin. The spot 1 from the high pH (low drip loss) sample (cf. Fig. 5) was excised from the gel and identified as α-actin (sequence coverage, 97%). The tryptic peptide (316–328) was identified at *m*/*z* 709.38 (2+) with a mass increment of 15 amu. Isolation of the precursor ion and MS/MS provided a series of characteristic b- and y-fragment ions from which the sequence, ^{316}EITALAPSTMKIK^{328} was identified with modification at Lys-326 to aminoadipic semialdehyde and at Met-325 to the sulfoxide (Fig. 7), preventing cleavage by trypsin. The comparison of MS/MS spectra of modified peptide (316–328)

Table 2
Carbonylated full length proteins identified by LC–MS after separation by 2D gel electrophoresis.

Band/spot	Protein	pI	Mw (KDa) gel	Peptides identified	Sequence coverage %	Protein accession no.
1[a]	Alpha-actin	5.3	42	47	77	P68137
2[a]	Tropomyosin	4.6	32	10	27	P07951
3[a]	Myosin light chain 1	4.9	21	18	29	P02602
4[a]	Myosin regulatory light chain 2	4.8	19	22	84	P97457
6[b]	Creatine kinase M chain	6.6	43	64	60	Q5XLD3
7[b]	GAPDH	5.8	38	23	41	P00355
8	Triosephosphate isomerase	6.4	26	54	69	Q29371
11	Carbonic anhydrase III	7.7	29	47	86	Q5S1S4
12	Adenylate kinase isoenzyme 1	8.7	21	23	52	P00571
13	Beta enolase	7.5	47	35	52	Q1KYT0
14	ATP synthase beta subunit	5.3	56	47	70	P11142
15	Heat shock cognate protein	5.3	71	42	58	P06576
16	Serum albumin	5.9	71	65	69	P08835

[a] Myofibrillar proteins.
[b] Sarcoplasmic proteins.

and unmodified peptide (316–326) cleaved after Lys-326 (Fig. 7A and B) provided evidence that the CID fragmentation of the peptide bond at Met-325 occurred at a higher rate for the modified peptide than for the unmodified tryptic peptide. The presence of y3 (−18) and the absence of y3 in the CID of the unmodified peptide suggested a cyclisation at Lys-326.

Protein spot 6 was identified as creatine kinase (90% sequence coverage). In the series of tryptic peptides, the fragment at *m*/*z* 832.45 (3+) was identified as (157–170) (LSVEALNSLTGEFK) with a mass increment of 156 amu. Modification at Lys-170 by 4-hydroxynonenal (HNE) was identified by tandem-MS analysis by a complete series of y*n*-ions (y1–y12) in comparison to the unmodified peptide, confirming the HNE moiety at Lys-170 (Fig. 6A and B). Remarkably, the modified Lys-170 residue is unaffected as a trypsin cleavage site. Corresponding HNE modifications have been previously identified in proteins at Lys, Cys and His residues [33,34]. Furthermore, oxidation of Trp-169 to the kynurenine derivative was identified in triosephosphate isomerase by the LC–tandem-MS analysis of the tryptic peptide (161–175) (shown in Supplementary Fig. S1).

4. Conclusions

Using a proteomics approach we have identified in this study postmortem changes in protein denaturation (decreased solubility) and oxidation by analyzing porcine muscle samples at different drip loss. By comparison of 2D-gel profiles of proteins from low and high drip loss, we could visualize changes in proteins even using Coomassie staining which was highly reproducible and was confirmed by silver-stained gels showing identical changes. Correlations of drip loss and protein carbonylations were identified by comparison of 2D-oxyblots. Predominantly, carbonylated proteins were found among myofibrillar proteins such as actin and isoforms of myosin, while sarcoplasmic proteins such as creatine kinase and triosephosphate isomerase showed no significant differences in their carbonylation level. Oxidative posttranslational modifications of myofibrillar proteins may be associated with important structural and functional alterations, such as impaired Ca^{2+} homeostasis and energy production in mitochondria [35,36].

High resolution FTICR-MS is shown here as a powerful tool for identification of truncated muscle proteins and isoforms, due to the low number of proteolytic peptides required for identification. Furthermore, the results of this study show that high resolution 2D-gel electrophoretic separation in combination with 2D-Western blot enable the sensitive detection of *post-mortem* protein denaturation and oxidation. The use of LC–MS/MS provided unequivocal identification of denatured and oxidized muscle proteins, and the determination of oxidative structure modifications. Thus, this methodology appears to be highly suitable for the detection and structural characterization of biomarker proteins.

Acknowledgements

We thank Reinhold Weber and Andreas Marquardt for expert assistance with the high resolution mass spectrometric analyses. This study has been supported by the Deutsche Forschungsgemeinschaft, Bonn, Germany (FOR-753).

Appendix A. Supplementary data

Supplementary data associated with this article can be found, in the online version, at doi:10.1016/j.ijms.2010.11.010.

References

[1] M. Koohmaraie, Biochemical factors regulating the toughening and tenderization processes of meat, Meat Sci. 43 (1996) 193–201.
[2] J. Huang, N.E. Forsberg, Role of calpain in skeletal-muscle protein degradation, Proc. Natl. Acad. Sci. U.S.A. 95 (1998) 12100–12105.
[3] M.E. Doumit, M. Koohmaraie, Immunoblot analysis of calpastatin degradation: evidence for cleavage by calpain in postmortem muscle, J. Anim. Sci. 77 (1999) 1467–1473.
[4] R. Lametsch, P. Roepstorff, E. Bendixen, Identification of protein degradation during post-mortem storage of pig meat, J. Agric. Food Chem. 50 (2002) 5508–5512.
[5] G. Offer, T. Cousins, The mechanism of drip production: formation of two compartments of extracellular space in muscle post-mortem, J. Sci. Food Agric. 58 (1992) 107–116.
[6] J.R. Bendall, J. Wismer-Pedersen, Some properties of fibrillar proteins of normal and watery pork muscle, J. Food Sci. 27 (1962) 144–159.
[7] R.D. Warner, R.G. Kauffman, M.L. Greaser, Muscle protein changes post-mortem in relation to pork quality traits, Meat Sci. 45 (1997) 339–352.
[8] K. Rosenvold, H.J. Andersen, Factors of significance for pork quality – a review, Meat Sci. 64 (2003) 219–237.
[9] R.N. Arnold, S.C. Arp, K.K. Scheller, S.N. Williams, D.M. Schaefer, Tissue equilibration and subcellular distribution of vitamin E relative to myoglobin and lipid oxidation in displayed beef, J. Anim. Sci. 71 (1993) 105–118.
[10] Sayre, D. Lin, Q. Yuan, Z. Zhu, X. Tang, Protein adducts generated from products of lipid oxidation: focus on HNE and ONE, Drug Metab. Rev. 38 (2006) 651–675.
[11] S.K. Jain, R. Yip, R.M. Hoesch, A.K. Pramanik, P.R. Dallman, S.B. Shohet, Evidence of peroxidative damage to the erythrocyte membrane in iron deficiency, Am. J. Clin. Nutr. 37 (1983) 26–30.
[12] F. Fenaille, J.C. Tabet, P.A. Guy, Identification of 4-hydroxy-2-nonenal-modified peptides within unfractionated digests using matrix-assisted laser desorption/ionization time-of-flight mass spectrometry, Anal. Chem. 76 (2004) 867–873.
[13] M. Renerre, K. Poncet, Y. Mercier, P. Gatellier, B. Métro, Influence of dietary fat and vitamin E on antioxidant status of muscles of turkey, Agric. Food Chem. 47 (1999) 237–244.
[14] R.L. Levine, J.A. Williams, E.R. Stadtman, E. Schacter, Carbonyl assays for determination of oxidatively modified proteins, Methods Enzymol. 233 (1994) 346–354.
[15] R. Plumb, J. Castro-Perez, L. Granger Beattie, K. Joncour, A. Wright, Ultra-performance liquid chromatography coupled to quadrupole-orthogonal time-of-flight mass spectrometry, Rapid Commun. Mass Spectrom. 18 (2004) 2331–1337.
[16] D. Galetskiy, I. Susnea, V. Reiser, I. Adamska, M. Przybylski, Structure and dynamics of photosystem II light-harvesting complex revealed by high-resolution FTICR mass spectrometric proteome analysis, J. Am. Soc. Mass Spectrom. 19 (2008) 1004–1013.
[17] D. Galetskiy, M. Woischnik, J. Ripper, M. Griese, M. Przybylski, Aberrant processing forms of lung surfactant proteins SP–B and SP–C revealed by high-resolution mass spectrometry, Eur. J. Mass Spectrom. 14 (2008) 379–390.
[18] R. Lametsch, A. Karlsson, K. Rosenvold, H.J. Andersen, P. Roepstorff, E. Bendixen, Post-mortem proteome changes of porcine muscle related to tenderness, J. Agric. Food Chem. 51 (2003) 6992–6997.
[19] F. Talamo, C. D'Ambrosio, S. Arena, P. Del Vecchio, L. Ledda, G. Zehender, L. Ferrara, A. Scaloni, Proteins from bovine tissues and biological fluids: Defining a reference electrophoresis map for liver, kidney, muscle, plasma and red blood cells, Proteomics 3 (2003) 440–460.
[20] A.G. Marshall, C.L. Hendrickson, G.S. Jackson, Fourier transform ion cyclotron resonance mass spectrometry: a primer mass, Spectrom. Rev. 17 (1998) 1–35.
[21] T.P. Conrads, G.A. Anderson, T.D. Veenstra, L. Pasa-Tolic, R.D. Smith, Utility of accurate mass tags for proteome-wide protein identification, Anal. Chem. 72 (2000) 3349–3354.
[22] G. Baykut, R. Jertz, M. Witt, Matrix-assisted laser desorption/ionization Fourier transform ion cyclotron resonance mass spectrometry with pulsed in-source collision gas and in-source ion accumulation, Rapid Commun. Mass Spectrom. 14 (2000) 1238–1247.
[23] P.K. Smith, R.I. Krohn, G.T. Hermanson, A.K. Mallia, F.H. Gartner, M.D. Provenzano, E.K. Fujimoto, N.M. Goeke, B.J. Olson, D.C. Klenk, Measurement of protein concentration using bicinchoninic acid, Anal. Biochem. 150 (1985) 76–85.
[24] C.R. Merril, D. Goldman, S.A. Sedman, M.H. Ebert, Ultrasensitive stain for proteins in polyacrylamide gels shows regional variation in cerebrospinal fluid proteins, Science 211 (1981) 1437–1438.
[25] E. Mortz, O. Vorm, M. Mann, P. Roepstorff, Identification of proteins in polyacrylamide gels by mass spectrometric peptide mapping combined with database search, Biol. Mass Spectrom. 23 (1994) 249–261.
[26] S. Bauer, M. Wiechers, K. Bruns, M. Przybylski, C. Stuermer, Isolation and Identification of the plasma membrane-associated intracellular protein Reggie-2 from Goldfish brain by chromatography and Fourier-transform ion cyclotron resonance mass spectrometry, Anal. Biochem. 298 (2001) 25–31.
[27] C. Conrad, J. Choi, C. Malakowski, J. Talent, R. Dai, P. Marshall, R. Gracy, Identification of protein carbonyls after two-dimensional electrophoresis, Proteomics 1 (2001) 829–834.
[28] G. Offer, P. Knight, R. Jeacocke, R. Almond, T. Cousins, J. Elsey, The structural basis of the water-holding, appearance and toughness of meat and meat products, Food Microstruct. 8 (1989) 151–170.

[29] G. Offer, Modelling of the formation of pale, soft and exudative meat: effects of chilling regime and rate and extent of glycolysis, Meat Sci. 30 (1991) 157–184.
[30] N. Kawashima, M. Mishima, R. Shindo, M. Hirano, S. Kuwabara, H. Saitoh, T. Miyazaki, Partial deficiency of phosphoglycerate mutase with diabetic polyneuropathy: the first Japanese patient, Intern. Med. 35 (1996) 799–802.
[31] A.M. Das, D.J. Byrd, Regulation of the mitochondrial ATP-synthase in skeletal muscle from children – a new diagnostic tool, J. Inherit. Metab. Dis. 19 (1996) 137–139.
[32] S.E. Harris, S.M. Huff-Lonergan, W.R. Lonergan, J. Jones, Rankins, Antioxidant status affects color stability and tenderness of calcium chloride-injected, J. Anim. Sci. 79 (2001) 666–677.
[33] Z. Liu, P.E. Minkler, L.M. Sayre, Mass spectroscopic characterization of protein modification by 4-hydroxy-2-(*E*)-nonenal and 4-oxo-2-(*E*)-nonenal, Chem. Res. Toxicol. 16 (2003) 901–911.
[34] K. Uchida, E.R. Stadtman, Selective cleavage of thioether linkage in proteins modified with 4-hydroxynonenal, Proc. Natl. Acad. Sci. U.S.A. 89 (1992) 5611–5615.
[35] B.M. Klebl, A.T. Ayoub, D. Pette, Protein oxidation, tyrosine nitration, and inactivation of sarcoplasmic reticulum Ca^{2+}-ATPase in low-frequency stimulated rabbit muscle, FEBS Lett. 422 (1998) 381–384.
[36] A. Kaasik, A. Minajeva, E. De Sousa, R. Ventura-Clapier, V. Veksler, Nitric oxide inhibits cardiac energy production via inhibition of mitochondrial creatine kinase, FEBS Lett. 444 (1999) 75–77.